

A COMPARATIVE ANALYSIS OF HYPOTHESIS IN THE MODELING OF A HYBRID COMPRESSION REFRIGERATION CYCLE

A. V. Clemente^a,
A. B. Lourenço^b,
R. G. Santos^{c,d},
and J. J. C. S. Santos^e.

^a Federal University of Espírito Santo - UFES
 Vitória, Brazil
 allan_vitor.c@hotmail.com

^b Federal University of Espírito Santo - UFES
 Vitória, Brazil
 atilio.lourenco@ufes.br

^c Federal Institute of Espírito Santo - IFES
 Vitória, Brazil

^d Federal University of Espírito Santo - UFES
 Vitória, Brazil
 rodrigo.guedes@ifes.edu.br

^e Federal University of Espírito Santo - UFES
 Vitória, Brazil
 jjcessantos@yahoo.com.br

Received: Ago 15, 2023

Reviewed: Ago 27, 2023

Accepted: Ago 30, 2023

ABSTRACT

This paper presents a comprehensive thermodynamic analysis of a hybrid refrigeration system that integrates an evacuated tube solar thermal collector into a vapor compression refrigeration cycle. The proposed analysis comprises two distinct approaches: an isovolumetric model and a compressible flow model. The former assumes a constant specific volume within the solar heat exchanger, while the latter applies principles of compressible fluid dynamics. The study compares these models with a reference work, emphasizing similarities and disparities. The investigation systematically varies key parameters, including evaporator and condenser temperatures, inlet and outlet temperatures of the heat exchanger, and heat load. By varying these parameters, the coefficient of performance (COP) and compressor work are evaluated, elucidating the impact of heat addition on the system's performance. Additionally, the influence of different working refrigerant fluids, such as R22 and R410A, is examined under various design point conditions. The results demonstrate the potential energy savings achievable by the hybrid system, with reductions in electrical power compared to the conventional compressor, as solar heat is introduced. While the isovolumetric analysis closely aligns with the reference work, the compressible flow modeling highlights sensitivity to inlet conditions. Although not directly comparable, the latter approach presents promising trends within specific design point ranges. Comparisons of performance curves for different refrigerant fluids further validate the models and assist in potential fluid selection. Overall, the outcomes indicate a promising avenue for energy-efficient refrigeration systems and provide valuable insights for engineering design and optimization.

Keywords: hybrid refrigeration system; evacuated tube solar thermal collector; energy savings; compressible flow modeling; refrigerant fluids

NOMENCLATURE

A	Area
COP	performance coefficient
C _p	specific heat
h	enthalpy
m	Mass
P	Pressure
Q	Heat
R	Gas Constant
s	Entropy
V	Speed
W	Compressor work
ρ	Specific mass

Subscripts

1	Thermodynamic state 1
2	Thermodynamic state 2
3	Thermodynamic state 3
4	Thermodynamic state 4
adc	Added
cond	Condenser
c	Conventional

evap	Evaporator
h	Hybrid
real	Real
s	Saved
x	Thermodynamic state x
o	Stagnation

INTRODUCTION

In the global context, the pursuit of more efficient systems that rely less on conventional energy sources has become a reality. According to a study published in the Proceedings of the National Academy of Sciences (cited in Instituto De Engenharia, 2018), one of the largest studies on the subject indicates that by 2040, increased use of air conditioning in hot climate regions will result in a 64% increase in electricity consumption and an annual increase of 23.1 million tons of carbon dioxide. According to Ministry of Mines and Energy (2018), in Brazil, considering only the energy efficiency measures already approved and publicized by the federal government, it is estimated that household electricity consumption for air conditioning could increase from 18.7 TWh in 2017 to

48.5 TWh in 2035, representing a growth of 5.4% per year during that period. It has been argued by Mehta and Rane (2013) that using solar energy for air conditioning is logical because the greater the availability of solar radiation, the higher the demand for air conditioning. This work presents a theoretical analysis of a refrigeration system with hybrid solar/mechanical compression. Encouraging values have been reported in studies, with savings ranging between 25% and 40% (Kumar and Patel, 2020). While only a few authors have contributed to the study of this system, some of their work is highlighted here. Brahmankar et al. (2018) conducted a comparative study between a conventional model and a hybrid model, assuming the refrigerant behaves as an ideal gas inside the solar exchanger, and obtained results close to 30% in energy savings. Assadi et al. (2016) also considered the gas as ideal and the volume constant in the evacuated tube exchanger, modeling the heat added to the system through the ANSYS-FLUENT software and suggesting a 25% energy saving if the air conditioning runs continuously for 24 hours. An experimental comparison approach was presented by Vakiloroaya et al. (2013), who monitored the thermodynamic states of a real plant and based their equation on the ideal gas condition. Ishak (2014) concluded that the system achieves a 30% energy saving compared to conventional systems, with a payback period of 3 years. Dhiraviam et al. (2017) studied temperature variations in the heat exchanger to maximize the COP. Yen (2015) conducted a more in-depth study on the solar thermal exchanger using the ANSYS software. Kumar and Patel (2020) presented an analysis based on the ideal gas hypothesis, developing the entire equation from it. This article intends to build upon these results and compare them with the findings presented here. The objective of this work is to propose two thermodynamic modeling approaches for the hybrid solar system under analysis, in order to provide further clarity on the process occurring in this counterintuitive system. According to information from Get Utilities, the company has completed over 6,000 commercial installations of such systems in three years (GET UTILITIES, 2023).

The first proposal models the inlet and outlet of the solar exchanger with a constant specific volume and assumes the gas behaves as an ideal gas. Intermittent analysis shows that adding heat under such conditions results in a pressure increase. This study offers a comparative analysis with Kumar and Patel (2020) using the same assumptions but different models.

The second proposal models the passage of the refrigerant through the solar exchanger as a compressible flow system. This hypothesis becomes highly relevant for the study because it directly influences the thermodynamic state in the system. In a supersonic compressible flow with added heat, an increase in outlet pressure relative to inlet pressure is observed. In short, adding heat in a supersonic compressible flow increases pressure, which is

desirable for analyzing the system in question. The study will focus on adjusting these velocities and states. The proposed approach is to model the system using the thermodynamic state library of the EES software, reducing its reliance on the ideal gas hypothesis, and proposing a new thermodynamic model for the solar thermal exchanger.

PHYSICAL STRUCTURE

The object of analysis in this study is a refrigeration system based on the vapor compression refrigeration cycle, featuring its four primary components: the evaporator, expansion valve, condenser, and compressor. The hybrid system distinguishes itself by incorporating an evacuated tube solar thermal collector, Fig. 1, between the compressor and the condenser. This arrangement has demonstrated the capability to globally decrease the electrical consumption of the system. As the fluid traverses the solar thermal exchanger, it absorbs heat and experiences a corresponding pressure elevation. This increase in pressure alleviates the demand on the compressor, thereby resulting in reduced electrical consumption. Although this system showcases improvements concerning electrical energy utilization, asserting that the system is inherently more energy-efficient would be inaccurate, given the additional heat energy being introduced. Nonetheless, the system's efficiency is evident when assessed solely with respect to electrical energy, as the load on the mechanical compressor is lessened when supplemented by the abundant and free energy source of the sun.

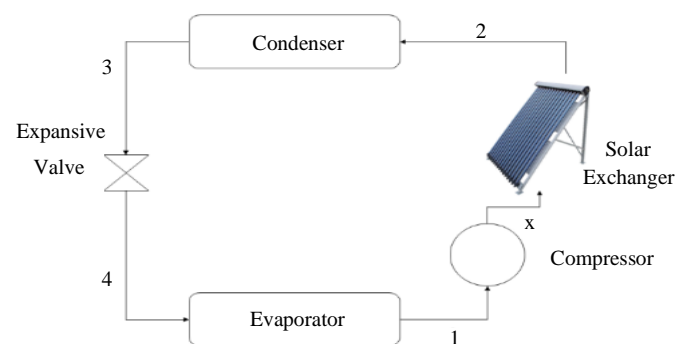


Figure 1 – Physical Structure

Thermodynamic modeling

The purpose of this study is to conduct a thermodynamic analysis of the process. The objective is to identify a model that adequately captures the essential characteristics of the actual system, with the intention of delineating the thermodynamic states prior to and following the evacuated solar exchanger.

Table 1. Input data

Evaporator Temperature	283 K
Condenser Temperature	312 K
Cooling Load	4,1 kW

The anticipated behavior of the hybrid system is delineated in Fig. 2b, illustrating the conceptual framework visually. This representation highlights the reduction in compressor demand from point 1 to 2 and the increased heat dissipation in the condenser from point 3 to 4. Figure 2a depicts the traditional system, and suggested values can be found in Table 1.

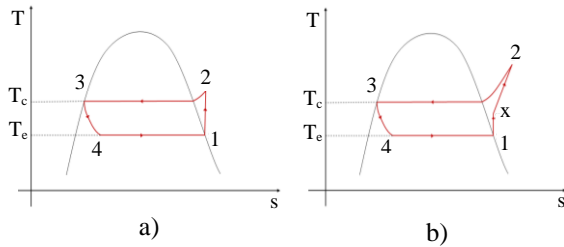


Figure 2. T x s diagram a) Conventional System b) Hybrid System

Mathematical equations

The energy conservation law for a given control volume can be described mathematically by Eq. 1 (Moran et al., 2009).

$$\dot{Q} - \dot{W} = \left(\frac{dE_{VC}}{dt} \right) + \dot{m}_{out} \cdot \left(h + \left(\frac{V^2}{2} \right) + gz \right)_{out} - \dot{m}_{in} \cdot \left(h + \left(\frac{V^2}{2} \right) + gz \right)_{in} \quad (1)$$

From the mathematical manipulation of the law of conservation of energy, combined with simplifying hypotheses, equations are obtained in simplified forms that define the entire ideal cycle, Fig. 2. The definition of the mass flow rate (\dot{m}) can be found by Eq. 2. The work on the compressor (\dot{W}_c), by Eq. 3. The coefficient of performance (COP_c), in the conventional system is estimated by the Eq. 4. For the hybrid system, Fig. 2b, one can observe some equations that differ from those already presented. The coefficient of performance in the hybrid system (COP_h) can be calculated by Eq. 5.

$$\dot{m} = \frac{\dot{Q}_{in}}{h_1 - h_4} \quad (2)$$

$$\dot{W}_c = \dot{m} \cdot (h_2 - h_1) \quad (3)$$

$$COP_c = \frac{(h_1 - h_4)}{(h_2 - h_1)} \quad (4)$$

$$COP_h = \frac{(h_1 - h_4)}{(h_x - h_1)} \quad (5)$$

On the other hand, the work on the hybrid system compressor (\dot{W}_h) is determined by Eq. 6, the saved

work (\dot{W}_s), by Eq. 7, and the ratio between the absorbed solar heat (\dot{Q}_n) by Eq. 8.

$$\dot{W}_h = \dot{m} \cdot (h_x - h_1) \quad (6)$$

$$\dot{W}_s = \dot{W}_c - \dot{W}_h \quad (7)$$

$$\dot{Q}_n = \frac{\dot{Q}_{adc}}{\dot{Q}_{adc_real}} \quad (8)$$

Approach admitting isovolumetric model

In this case, two approaches to thermodynamic analysis will be examined. In the first approach, the analysis occurs between states 2 and 3, corresponding to the input and output, respectively, of the evacuated tube exchanger. This analysis maintains a constant specific volume, which is derived from the EES software library. The modeling involves setting the heat exchanger outlet pressure to match the pressure inside the condenser in the conventional cycle. Additionally, the inlet pressure (P_2) for the heat exchanger is determined using the EES software state library, in conjunction with an equation derived from the first law of thermodynamics. Equation 9 is employed to estimate the enthalpy of state "x".

$$h_x = h_2 - \frac{\dot{Q}_{adc}}{m} \quad (9)$$

Approach admitting supersonic compressible flow

In this approach, the problem is presumed to be analogous to a Rayleigh problem, entailing specific underlying assumptions. The heat exchanger process is modeled as a frictionless compressible flow, wherein the section maintains a continuous area. Additionally, a pivotal assumption is that the refrigerant conforms to the properties of an ideal gas. For this, the Compression Factor is assessed for each state of the refrigerant, aligning with a parameter that approximates ideal gas behavior. By utilizing the equation pertinent to the Rayleigh Problem, it becomes apparent that the momentum equation facilitates the determination of velocity in state 2 (V_2), by Eq. (10). The Mass equation (Eq. 11) was used to define the density of state 2 (ρ_2). Equation 12 to define T_2 . Here, M represents the Mach number in the fluid, and k denotes the adiabatic expansion coefficient at the stagnation temperature, as shown in Eq. (13).

$$V_2 = V_1 + \left(\frac{P_2 - P_1}{\rho_1 \cdot V_1} \right) \quad (10)$$

$$\rho_2 = \left(\frac{m}{A \cdot V_2} \right) \quad (11)$$

$$T_2 = \left(\frac{P_2}{\rho_x \cdot R} \right) \quad (12)$$

$$T_{02} = T_2 \cdot M_2^2 \cdot \left(1 + \frac{k-1}{2} \right) \quad (13)$$

The enthalpy at state 2 (h_2), along with all other state 2 parameters, is currently determined using the EES Software library. Where (c_p) is the specific heat, the stagnation temperature at x (T_{0x}) is given by Eq. 14. To set the temperature in x (T_x), was used Eq. 15. The enthalpy at x (h_x) is then defined by the isentropic efficiency (η), the state x isentropic (h') and the enthalpy at 2 (h_2) by the Eq. 16.

$$T_{0x} = T_{02} + \left(\frac{Q \cdot c_p}{m} \right) \quad (14)$$

$$T_x = \frac{T_{0x}}{\left(1 + \left(\frac{k-1}{2} \right) \right) \cdot M_2^2} \quad (15)$$

$$h_x = \left(\frac{h' - \eta \cdot h_2}{1 - \eta} \right) \quad (16)$$

With two properties of state x now at our disposal, it will also be determined using the EES Software library. The velocities in the states are defined by the mass equation. Once the mass flow is known and the specific mass is defined in each state, the area of the flow section is determined based on the guidelines provided in this work. The Rayleigh problem establishes that for subsonic flows at the inlet of a frictionless heat exchange pipe, the Mach number will progressively increase along the pipe until it reaches the maximum value of $M=1$ when heat is added, leading to a subsequent reduction in pressure. However, in the case of flows with inlet velocities surpassing the speed of sound, the Mach number will decrease to $M=1$ upon heat addition, causing an inverse effect on pressure a consequential increase. This approach is reasonable given that, for the refrigerant fluids under examination, the states in which they are evaluated theoretically allow the speed of sound propagation to be attainable within the solar exchanger. While Rayleigh modeling is employed to simulate Scramjet engines, enhancing model reliability, its applicability is limited for comparative purposes in this study. This limitation stems from the fact that Scramjet engines model air as the gas, which contrasts with the refrigerant fluids investigated here. Thus far, no instances have been identified wherein the Rayleigh problem has been utilized to model this hybrid refrigeration system.

RESULTS AND DISCUSSIONS

The two proposed thermodynamic models for this study will undergo evaluation. The first model involves maintaining a constant specific volume within the solar heat exchanger, while the second model considers compressible flow and accordingly models the system. Subsequently, several working fluids will be assessed for both analyses. In each analysis, the outcomes and a preliminary analysis of these results will be presented.

Constant volume

The first analysis involves a comparison between the model proposed in this study, which assumes a constant volume inside the evacuated tube solar thermal heat exchanger, and the model presented by Kumar and Patel (2020). In pursuit of this objective, graphs were formulated using identical parameters to facilitate the comparison of the two approaches. This process aims to stimulate discussions regarding the disparities between the two models. It's worth reiterating that the reference work by Kumar and Patel (2020) also adopted the assumption of a constant volume inside the solar heat exchanger. However, a significant distinction arises in that their study's data and parameters were validated and tested against a physical model of the system, involving real-world experiments. To create these graphs, four key parameters were entered, all grounded in the reference article: the temperature within the evaporator (T_{evap}), the condenser's outlet temperature (T_{cond}), the temperature at the outlet of the solar heat exchanger (T_2), and the cooling effect in the evaporator (\dot{Q}_{evap}). Temperature was measured in Kelvin, while cooling was quantified in kilowatts (kW). The initial parameters employed for this modeling endeavor are delineated in Table 1. Subsequently, the three aforementioned temperatures were systematically varied and plotted on each graph, while the cooling remained consistently set at 4.1 kW.

Temperature variation in the solar exchanger

In the initial analysis, as depicted in Fig. 3a and 3b, the temperatures of the evaporator and condenser were set, and the temperature at state 2 was systematically varied. This procedure enabled the evaluation of the coefficient of performance (COP) and compressor work for both the conventional and hybrid systems. The COP and compressor work in the conventional system remained constant throughout the analysis, while the COP in the hybrid system exhibited fluctuations. Upon comparing these results with the corresponding graphs presented in the work by Kumar and Patel (2020), minor deviations can be observed. These differences are likely attributed to the adoption of distinct models. "Nevertheless, the underlying curve trend remains similar, indicating model equivalence. This consistent pattern aligns with the anticipated system behavior: higher heat exchanger

outlet temperatures increase heat influx, enhancing the system's COP and saving on compressor work.

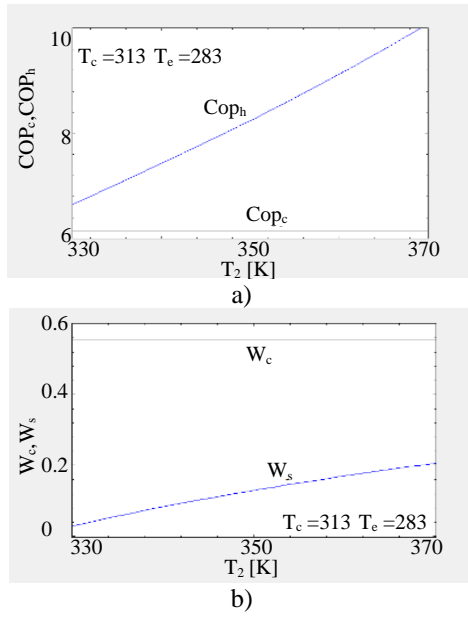


Figure 3. Relationship between solar exchanger outlet temperature and a) COP b) Compressor work

Temperature variation in the evaporator

As depicted in Figures 4a and 4b, the focus shifts to varying the evaporator temperature, allowing for a comprehensive evaluation of its influence on the coefficients of performance (COPs) and compressor work in both systems.

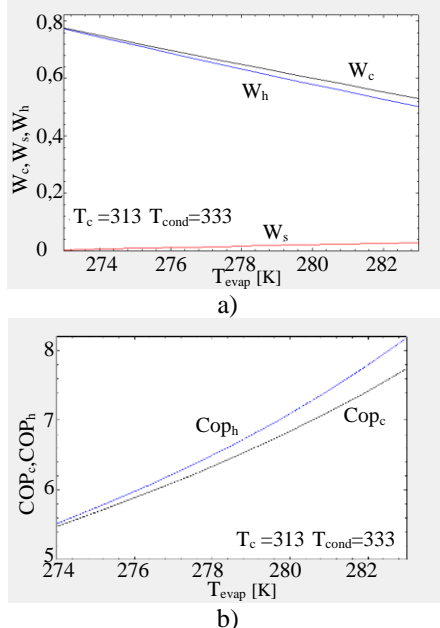


Figure 4. Relationship between Evaporator Temperature and a) Compressor Work b) COP.

Similar to the findings in the initial analysis, the results of this analysis also exhibited minor variations in values, yet they consistently adhered to the same underlying pattern and curve trajectory. Specifically, an elevation in the evaporator temperature yielded an increase in the coefficient of performance (COP) and a decrease in the work required, demonstrating a consistent trend across the evaluations.

Temperature variation in the condenser

In the subsequent analysis, depicted in Fig. 5a and 5b, the focus is shifted towards varying the temperature within the condenser.

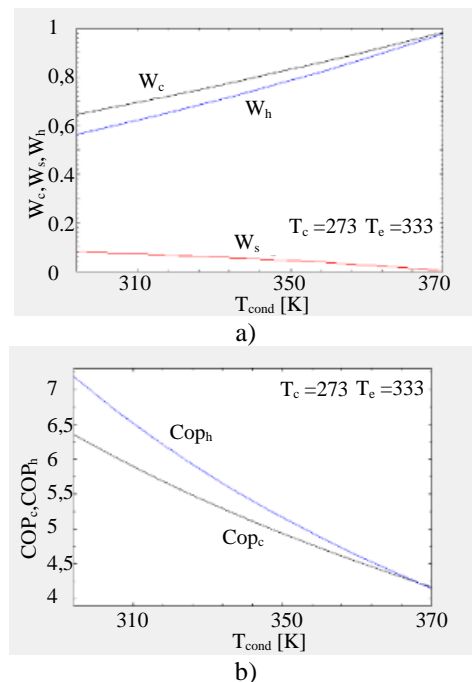


Figure 5. Relationship between Condenser Temperature and a) Compressor Work b) COP

This variation maintains the same approach of comparison and evaluation as in the previous analyses.

Compressible flow

This modeling approach introduces a higher level of complexity, both in terms of its equations and the resulting outcomes. Initially, when inputting the parameters from the constant volume model, as listed in Table 1, into the EES software, the code encountered convergence issues. Consequently, it was not feasible to generate comparative graphs between the two models. However, it is important to note that similar challenges were encountered in the comparison study by Kumar and Patel (2020) with their real physical model. In order to achieve substantial savings in their model, they needed to incorporate an additional component – a solenoid

valve – to control the fluid output from the solar exchanger. This implementation favored the isovolumetric modeling approach, as the valve's closure restricted the passage and maintained a constant volume within the solar exchanger. While this solution represents a technological adaptation to the issue, no instances were found in the available literature where such an approach had been adopted. This does not undermine the credibility of the article; it merely reflects the specific method chosen by the authors to effectively model the problem. However, this situation directs attention to the compressible flow model, which has demonstrated that under free flow conditions, the input parameters selected may not yield satisfactory energy-saving results. The compressible flow modeling is directly influenced by both the flow velocity and the thermodynamic state at the entrance of the solar exchanger, in accordance with existing literature (Fox et al., 2006). This implies that for a pressure increase during compressible flow with the addition of heat, the inlet velocity must exceed Mach 1 under inlet conditions. However, given the chosen values for the tubular section area and the adopted thermal load (cooling), the inlet velocity within the heat exchanger fell short of reaching Mach 1.

Table 2. Initial data for compressible flow

Evaporator Temperature	283 K
Condenser Temperature	312 K
Tubular section area (Solar Exchanger)	0,00023 m ²
Pressure in X	P ₂

Consequently, an analysis was conducted on Fig. 6, depicting the Mach analysis at the entry point of the solar exchanger in relation to the thermal load of the evaporator. This assessment was based on the input data outlined in Table 2. To assess the tubular section area within the solar exchanger and establish parameters for defining an appropriate area value for the real model's operation, a study was conducted as illustrated in Fig. 7.

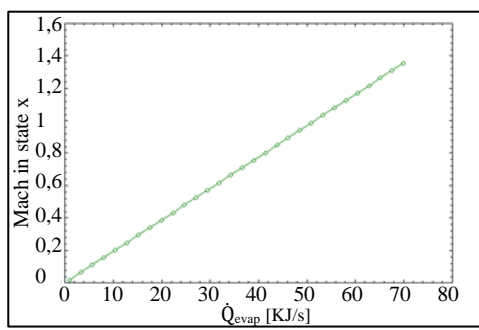


Figure 6. Mach x Thermal Load

This investigation involved examining the behavior of Mach in relation to the tubular section area. The analysis employed the same parameters as specified in Table 1, along with the identical thermal

load (cooling) as utilized in the comparative work by Kumar and Patel (2020) with $\dot{Q}_{evap} = 4.1$ kW.

From Fig. 7, it becomes evident that Mach reaches a value of approximately 1 when the area is equivalent to 0.000016 m². This observation implies that the model can achieve adequate flow velocities when employing areas smaller than this threshold. It is crucial to note that the assessment of whether these values are physically achievable is beyond the scope of this study. While a multitude of analyses could be performed by varying parameters and exploring a broad range of conditions wherein the compressible flow model might function effectively, this study has focused on adhering to the original analysis conditions outlined in Table 2. The approach involves allowing the pressure at point x to vary freely, while utilizing thermal load values of 60 kW. With this approach, the work executed by the compressor and the system's COP will be evaluated and compared in the context of the hybrid system and the conventional system conditions.

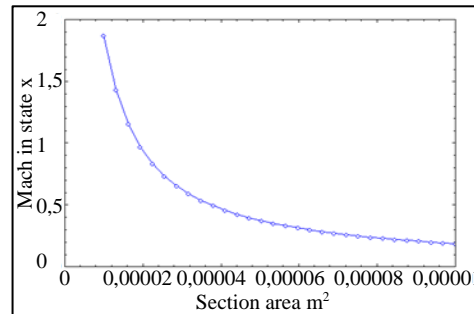


Figure 7. Mach x Section Area

In the context of this modeling, the heat injected into the system through the evacuated tube exchanger is denoted as \dot{Q}_{adc} . Its calculation is determined by Eq. 15. This parameter was subjected to variation, serving as the controlled parameter for the analysis presented in Fig. 8a and 8b. The objective of this analysis was to assess the impact of varying \dot{Q}_{adc} on key performance parameters such as COP and the compressor's workload. All other parameters utilized in the analysis are specified in Table 2, except for the pressure at point x. Figure 8a and 8b portray the outcomes of this variation in heat injection. The presented graphs provide insights into how COP and the compressor's work evolve as \dot{Q}_{adc} is altered. The deliberate manipulation of \dot{Q}_{adc} enables an exploration of the system's behavior under diverse thermal load conditions, ultimately contributing to a comprehensive understanding of the system's performance characteristics.

The conducted analysis demonstrates consistent trends akin to the analyses performed under the constant volume hypothesis. The hybrid system's COP (COP_h) exhibits an increase compared to the COP of the conventional system. Simultaneously, as anticipated, the compressor's work (\dot{W}_h) decreases in

the hybrid system, leading to greater energy savings, whereas the work of the conventional system remains steady. This analysis effectively illustrates the system's response as heat is introduced to the evacuated solar exchanger, aligning with anticipated outcomes. The utilization of the ideal gas assumption is pivotal for the modeling endeavor. However, a thorough investigation of this assumption is essential. To address this, a comparative study was conducted between the heat introduced into the solar exchanger modeled with the constant specific heat capacity (C_p) equation (Eq. 15) and the heat calculated by the EES software.

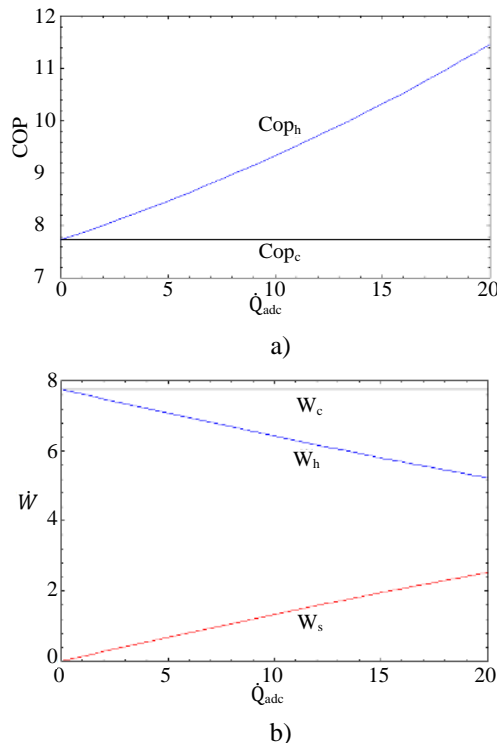


Figure 8. Added Heat in the Solar Exchanger and a) COP b) Work on the Compressor

The software defined the heat using the enthalpies of states x and 2 as parameters through Eq. (13). The relationship between these two quantities, as encapsulated by Eq. 8 (Q_n), facilitated the derivation of the percentage difference between them. Figure 14 showcases the outcomes of this comparison. In addition, the compressibility factor was assessed for each unit of heat introduced into the solar exchanger, as it serves as an indicator of a gas's deviation from ideal behavior. The values of Q_n reveal that the disparity between theoretical heat and actual heat remains below 20%, and this discrepancy diminishes as the compressibility factor rises, particularly in the range of 0.7 to 0.8. However, a more intricate examination is warranted to determine the adequacy of these results. As illustrated in Fig. (10), a simulation

was conducted under identical conditions, but with a fixed quantity of 10 kW of heat absorbed in the solar exchanger. The graph's lines assume a polygonal form due to the software's depiction of discrete points on the dome, connected by straight lines. Notably, the lines align closely with the anticipated outcome, as depicted in Fig. 2b, suggesting a convergence between the theoretical model and the simulated results.

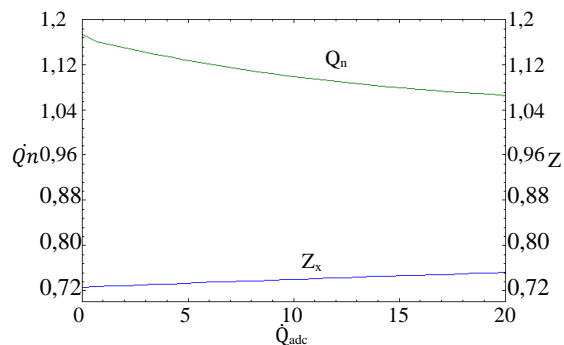


Figure 9. Evaluation of the ideal gas hypothesis

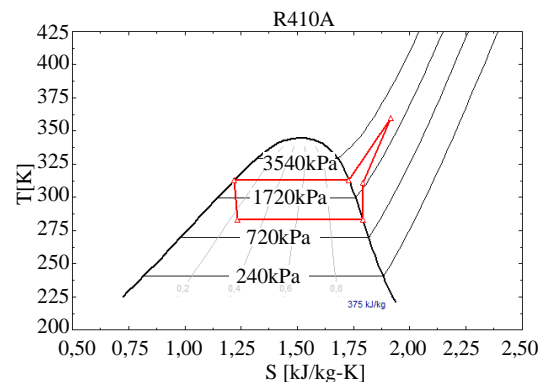


Figure 10. Real TxS diagram

Comparison of different working fluids

A comparative analysis of different working fluids was also conducted, as depicted in Fig. 11a and 11b. These figures present an assessment of the behavior of the hybrid Coefficient of Performance (COP) for the system, while adhering to their respective modeling approaches. In the compressible flow modeling, the effect of varying the heat added to the system via the hybrid solar exchanger was explored, revealing that the refrigerant fluid R22 outperformed R410A in terms of the compressible flow model, as depicted in Fig. 11a. On the other hand, in the constant volume modeling, the analysis focused on varying the outlet temperature of the heat exchanger. Interestingly, all three evaluated fluids displayed similar performance under these conditions. It's worth noting that the evaluation conditions were not identical between the two scenarios, as depicted in Fig. 11a and 11b. Fig. 11a used a 60 kW heat load, and

Fig. 11b employed a 4.1 kW heat load, matching their modeling approaches.

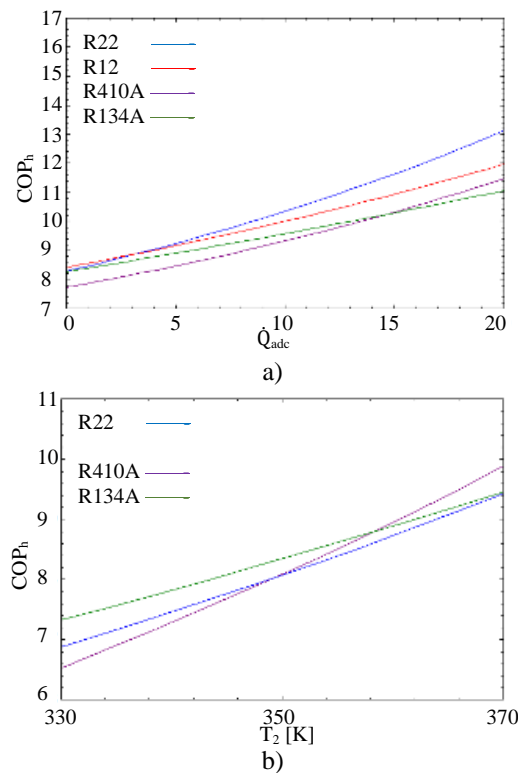


Figure 11. Evaluation of Fluids for a) compressible flow b) Constant volume

CONCLUSION

In conclusion, the hybrid refrigeration system showed potential for energy savings by significantly reducing electrical energy consumption in the conventional compressor when heat is integrated via the solar thermal exchanger. The isovolumetric analysis in this study yielded results similar to Kumar and Patel (2020), albeit with minor differences due to methodology variations, including the use of EES software properties versus ideal gas equations. Despite these differences, the trends in the curves indicate a degree of equivalence between the models. However, the analysis based on compressible fluid modeling didn't align entirely with available comparison models. This inconsistency can be attributed to the sensitivity of compressible fluid modeling to inlet conditions, such as flow area and thermal load. While it provided valuable insights within specific operating conditions, further investigation is needed for validation against real-world or mathematically defined models with appropriate initial conditions. The comparison of performance curves among different refrigerant fluids supported the validation of the models, as consistent trends were observed. In summary, the results, although subject to limitations, were generally in line with the expected outcomes of this study.

ACKNOWLEDGEMENTS

The authors thanks to FAPES, UFES, IFES, CAPES, and CNPq.

REFERENCES

Assadi, MK, Gilani, SI, & Yen, TJ 2016. *Design of a solar hybrid air conditioning compressor system*. In MATEC Web of Conferences (Vol. 38, p. 02001). EDP Ciências.

Brahmankar, C., Bhushan, H., Ghule, A., & Ranjan, H., 2018. *Study of hybrid split air conditioning assisted by solar thermal collectors*. International Journal of Engineering and Technology Research (IRJET) , 5 (4).

Dhiraviam, F. J., Naveenprabhu, V., & Santhosh, M. 2017. *Study the Effects of Solar Assisted Vapour Compression Air Conditioning System for Winter Applications*. International Journal for Scientific Research & Development, 4(11), 505-508.

Fox, R. W., McDonald, A. T., & Pritchard, P. J., 2006. *Introduction to Fluid Mechanics*, 6^a edição. LTC Editora. Pg. 650.

GET UTILITIES, *A refrigeração e ar condicionado com maior eficiência energética do planeta*, <https://getutilities.ie/solarcool>

INSTITUTO DE ENGENHARIA, 2018. <https://www.institutodeengenharia.org.br/site/2018/05/18/ar-condicionado-deve-triplicar-a-demanda-por-energia-ate-2050/> acessado em 12/2019

Ishak, A. R. B. 2014. *Study of hybrid solar air conditioning*. Universiti Teknologi Petronas, 14983

Kumar, MA, & Patel, D. (2021). *Evaluation of the performance and thermodynamics of a hybrid solar air conditioning system*. Materials Today: Anais , 46 , 5632-5638.

Mehta.J. R, M. V. Rane. *Liquid desiccant based solar air conditioning system with novel evacuated tube collector as regenerator*, 2013=

Ministério de Minas e Energia, Nota Técnica EPE 030/2018, 2018

Moran, M. J., Shapiro, H. N., Boettner, D. D., & Bailey, M. B., 2009. *Principles of Thermodynamics for Engineering*, 6^a edição. Rio de Janeiro: Editora LTC.

Vakiloroaya, V., Ha, QP, & Skibniewski, M., 2013. *Experimental modeling and validation of a solar-assisted direct expansion air conditioning system*. Energia e Edifícios , 66 , 524-536.

Yen, T. C. J. 2015. *Design a solar hybrid air conditioning compressor system*. Universiti Teknologi Petronas. 14982.